

Relaxed Equivariant Graph Neural Networks

Elyssa Hofgard¹ Rui Wang¹ Robin Walters² Tess Smidt¹

Abstract

3D Euclidean symmetry equivariant neural networks have demonstrated notable success in modeling complex physical systems. We introduce a framework for relaxed $E(3)$ graph equivariant neural networks that can learn and represent symmetry breaking within continuous groups. Building on the existing $e3nn$ framework, we propose the use of relaxed weights to allow for controlled symmetry breaking. We show empirically that these relaxed weights learn the correct amount of symmetry breaking.

1. Introduction

3D Euclidean symmetry equivariant neural networks or $E(3)$ NNs (Cohen & Welling, 2016; Thomas et al., 2018; Kondor, 2018; Weiler et al., 2018) have had considerable success in modeling complex physical data—from learning ab initio molecular dynamics (Batzner et al., 2022) to predicting quantum mechanically accurate properties of molecules and crystals (Rackers et al., 2023; Fang et al., 2024). Through integrating physical symmetries into the model architecture, equivariant neural networks can achieve superior generalization and data efficiency (Liao et al., 2023; Batzner et al., 2022; Frey et al., 2023; Rackers et al., 2023; Owen et al., 2023).

However, in many physical settings, there may be symmetry breaking or approximate symmetries. For instance, in crystal phase transitions, spontaneous symmetry breaking marks the shift from a high-symmetry state (like a liquid) to a low-symmetry, ordered crystalline structure, fundamentally altering the material’s properties. Symmetry breaking can also occur when external forces act on the system. For example, in fluid dynamics, external forces or temperature gradients can break the Euclidean symmetry of a uniform

¹Department of Electrical Engineering and Computer Science, MIT, USA ²College of Computing Sciences, Northeastern University, USA. Correspondence to: Elyssa Hofgard <ehofgard@mit.edu>.

Proceedings of the Geometry-grounded Representation Learning and Generative Modeling at 41st International Conference on Machine Learning, Vienna, Austria. PMLR Vol Number, 2024. Copyright 2024 by the author(s).

fluid layer (Tagawa, 2023). It is therefore desirable to develop models capable of parametrizing sources of symmetry breaking for applications across diverse physical systems. In this work, we refer to these sources of asymmetry as symmetry-breaking factors. It is noteworthy that these factors are analogous to order parameters in Landau theory, which describe the system parameters leading to phase transitions (Landau, 1936). Previous works (Wang et al., 2022; 2024) have developed relaxed group convolutions for discrete groups to learn and parametrize symmetry breaking. We develop a relaxed equivariant graph convolution neural network architecture, generalizing to the continuous group $E(3)$ using operations present in $e3nn$ (Geiger et al., 2022; Geiger & Smidt, 2022).

2. Background

We begin with a brief overview of the group representation theory and notation relevant to convolutions in $E(3)$ equivariant neural networks. Euclidean symmetry in 3D includes 3D translations, rotations, and inversion. Translation equivariance is typically achieved by using convolutions. Convolutional filters are thus constrained to be equivariant to $O(3) = SO(3) \times \mathbb{Z}_2$, the group of 3D rotations and inversion. In the following sections, we thus discuss $O(3)$.

Group representations. Group representations provide a concrete way to handle abstract symmetry groups. A representation of a group G on vector space V of dimension d is a function $D : G \rightarrow \text{GL}(V)$. $\text{GL}(V)$ is the group of invertible $d \times d$ matrices. A representation D has the following properties $\forall g, h \in G$ and where $e \in G$ is the identity element: (i) $D(gh) = D(g)D(h)$ and (ii) $D(g)D(g^{-1}) = D(g^{-1})D(g) = D(e) = \mathbf{I}_d$.

Irreducible representations. An irreducible representation (irrep) is a representation that does not contain a smaller representation—there is no nontrivial projector $P \in \mathbb{R}^{q \times d}$ such that $g \rightarrow PD(g)P^T$ is also a representation (Dre, 2008). In $E(3)$ NNs, data is typed by how it transforms under given irreps.

The irreps of $O(3)$ are the product of the irreps of $SO(3)$ and \mathbb{Z}_2 . For $SO(3)$, the irreps are indexed by a positive integer angular frequency $l = 0, 1, 2, \dots$. For \mathbb{Z}_2 , there are two irreps: the even irrep indexed by parity $p = 1$ and the odd irrep indexed by parity $p = -1$. The irreps of $O(3)$

thus carry both l and p indices and can be associated with matrices $D^{l,p}$. Each irrep has an associated matrix $D^{l,p}$ which operates on the vector space V^l of dimension $2l+1$. In this work, we will use tuples (l, p) and symbols l_p to indicate specific irreps. The former is useful when dealing with tensor indices and the later is easier when explicitly listing direct sums or concatenations of irreps.

Spherical harmonics. Convolutions that are equivariant to $O(3)$ are built from spherical harmonics. The spherical harmonics are a family of functions Y^l from the unit sphere to the vector space of the irrep $D^{l,p}$, $Y^l : S^2 \rightarrow V^l$, and form a basis for all equivariant polynomials on the sphere (Geiger & Smidt, 2022). The $2l+1$ spherical harmonics for a given l are denoted by Y_m^l where $m = -l, \dots, 0, \dots, l$. The spherical harmonics have specific parity, with even l spherical harmonics being even under inversion ($p = 1$) and odd l spherical harmonics being odd under inversion ($p = -1$). The spherical harmonics are equivariant under $O(3)$ and thus transform via $D^{l,p}$:

$$Y_m^l(R(g)\vec{r}) = D^{l,p}(g)_{mk} Y_k^l(\vec{r}) \quad (1)$$

where \vec{r} is a 3D vector and R is the representation of $O(3)$ on 3D vectors (a rotation matrix).

E(3) equivariant graph convolutions. The primary distinction between traditional convolutions and equivariant convolutions lies in the operations between filters and inputs. Equivariant convolutions must ensure that any operation respects underlying symmetries and faithfully treats higher-order geometric objects (beyond scalars). $E(3)$ NNs thus use tensor product decompositions.

Tensor product decompositions multiply two direct sums of irreps (input and filter) and provides the change of basis back into a new direct sum of irreps (output) in way that preserve the multiplication rules of the group. The product of two irreps can produce multiple different irreps, referred to as different “paths” of interaction that are independently equivariant. At a high level, these tensor product decompositions are encoded by a three index tensor built from Clebsch-Gordan coefficients. For two inputs x and y , $x \otimes y = \sum_{\alpha\beta} C_{\alpha\beta\gamma} x_\alpha y_\beta = z$ such that we are guaranteed the property that $D^Z(g)z = D^X(g)x \otimes D^Y(g)y$. See Geiger & Smidt (2022) for more detail.

While in Thomas et al. (2018); Kondor (2018); Weiler et al. (2018), the convolutional filter is expressed in terms of a radial basis multiplying the spherical harmonics, in more recent networks such as those implemented in e3nn, radial functions are used to provide weights to the tensor product decomposition, as each independent “path” can be weighted by a scalar and still preserve equivariance (Geiger & Smidt, 2022). We adopt the following notation for equivariant

convolutions.

$$\tilde{Y}(\hat{r}_{ab}) = \bigoplus_{l=0}^{l_{\max}} Y_l(\hat{r}_{ab}) \quad (2)$$

$$f'_a = \frac{1}{\sqrt{N}} \sum_{b \in \delta(a)} f_b \otimes_{W(||r_{ab}||)} \tilde{Y}(\hat{r}_{ab}) \quad (3)$$

f_b, f'_a are the input and output node features. N is the average degree of the nodes, \hat{r}_{ab} is the relative unit vector from position a to b , $\delta(a)$ is the set of neighbor nodes of node a , and \tilde{Y} is the entire set of spherical harmonics used in the filter from $l = 0$ to some l_{\max} . The spherical harmonic projection $\tilde{Y}(\hat{r}_{ab})$ refers to evaluating the spherical harmonics at \hat{r}_{ab} at each $Y^l, 0 \leq l \leq l_{\max}$ and concatenating the results. The learnable radial function that parameterizes the tensor product $W(||r_{ab}||)$ is a multi-layer perceptron (MLP) acting on a set of b radial basis functions $B : \mathbb{R} \rightarrow \mathbb{R}^b$ evaluated at the magnitude $||r_{ab}||$. W has the form:

$$W := \text{MLP}(B(||r_{ab}||)_{((c,l,p)_i, (c,l,p)_f, (c,l,p)_o)}) \quad (4)$$

where c indicate channel indices, as there can be multiple copies of a given irrep in the input or output. (l, p) with indices i, f, o specify the irreps in the input, filter, and output respectively. Tallowed combinations of l_i, l_f , and l_o are determined by the group multiplication rules (Clebsch-Gordan Coefficients). Common choices of radial basis functions include evenly space, partially overlapping Gaussians or Bessel functions. In our work, we expand upon this $E(3)$ equivariant graph convolution.

3. Related Work

Wang et al. (2022) proposed relaxed group convolution for discrete groups. Wang et al. (2024) extended relaxed group convolutions to show that they can allow the model to maintain the highest level of equivariance consistent with the data and discover symmetry-breaking factors. We propose a formulation of relaxed convolutions for continuous rather than discrete groups. Smidt et al. (2021) demonstrated that the gradients to ENNs can be used to learn the appropriate symmetry breaking factors through providing an additional trainable input. Our approach is complimentary in that we allow the weights to break symmetry rather than training an additional input to the network. McNeela (2023) proposes a Lie algebra convolution to relax the equivariance bias but does not show how to recover symmetry breaking factors.

4. Methodology

4.1. Definition of relaxed $E(3)$ NN

Here, we present the definition of our **relaxed $E(3)$ equivariant graph neural network** or relaxed $E(3)$ NN. The relaxed

weights $\tilde{\theta}$ are the direct sum or concatenation of scalar and non-scalar irreps (which if non-zero break $O(3)$ symmetry). For example, if we wanted to include all irreps up to some angular frequency cutoff l_{relaxed} , $\tilde{\theta}$ would be

$$\tilde{\theta} = \bigoplus_{\substack{0 \leq l \leq l_{\text{relaxed}} \\ p \in \{1, -1\}}} \theta^{l,p} \quad (5)$$

where l and p indicate the angular frequency and parity of the irrep of $O(3)$, respectively. As irreps are $2l + 1$ dimensional, the overall dimensionality of $\tilde{\theta}$ depend both on the number and types of non-scalar irreps it is built from. We interact our learned relaxed weights with the spherical harmonic projection of relative distance vectors via a tensor product $\tilde{\theta} \otimes \tilde{Y}(\hat{r}_{ab})$. The full equation for relaxed convolution is then

$$f'_a = \frac{1}{\sqrt{z}} \sum_{b \in \delta(a)} f_b \otimes_{W(||r_{ab}||)} (\tilde{\theta} \otimes \tilde{Y}(\hat{r}_{ab})) \quad (6)$$

The weights that parameterize the tensor product of the filter and input $W(||r_{ab}||)$ now depend on the direct sum of irreps formed by the tensor product of $\tilde{\theta} \otimes \tilde{Y}(\hat{r}_{ab})$. Note that the relaxed weights are shared across input and output channels, thus only introducing a few more parameters for each layer.

We initialize the relaxed weights $\tilde{\theta}$ such that the initial model remains equivariant to ensure the model learns the minimal amount of symmetry breaking.

Proposition 4.1. *The relaxed $E(3)$ NN is equivariant if and only if $\tilde{\theta}$ transforms as a scalar, i.e. only the term corresponding to the scalar irrep is non-zero.*

Proof. For the relaxed $E(3)$ NN to be equivariant, the following must be true

$$D^{\tilde{\theta} \otimes \tilde{Y}}(\tilde{\theta} \otimes \tilde{Y}(\hat{r}_{ab})) = (\tilde{\theta} \otimes \tilde{Y}(R(g)\hat{r}_{ab})) \quad (7)$$

This can only be true for any $D^{\tilde{\theta} \otimes \tilde{Y}}$ if $\tilde{\theta}$ transforms as a scalar. \square

We thus initialize $\tilde{\theta}$ such that only the scalar irrep is non-zero. We emphasize that pseudoscalars, $\theta^{0,-1}$ change sign under inversion in $O(3)$ and are thus non-scalar irreps.

4.2. Interpreting Relaxed Weights as Spherical Signals

This definition of relaxed weights also provides interpretability. As spherical harmonics form the basis for functions on a sphere, irreps representing symmetry breaking can be visualized as scalar or pseudoscalar signals illustrating the amount of symmetry or asymmetry learned by the relaxed

weights. The scalar signal would be given by

$$f(\vec{x}) = \sum_{\substack{0 \leq l \leq l_{\text{relaxed}} \\ p = \{\text{parity}(Y^0), \dots, \text{parity}(Y^{l_{\text{relaxed}}})\}}} \theta^{l,p} \cdot Y^l(\vec{x}) \quad (8)$$

where we sum over relaxed weights with the same parity as the spherical harmonics. The pseudoscalar signal would be given by summing over relaxed weights with opposite parity to the spherical harmonics.

5. Experiments

We present experiments showing that the relaxed $E(3)$ NN learns the correct symmetry breaking factors. Smidt et al. (2021) noted that the output of an equivariant neural network will always be higher than or equal symmetry than an input. Thus, without the addition of relaxed weights or a trainable input parameter, one will not be able to deform a shape with higher symmetry into a shape with lower symmetry for example.¹ Model details are in Appendix B.

5.1. Shape Deformations

We consider deformations of 3D shapes, expressed in points of the form (x, y, z) . The network takes as input the spherical harmonic projection of the vertices of the initial shape and aims to produce, as output, the spherical harmonic projection of the vertices of the transformed shape, up to some specified l_{max} . We deform a cube to a cube, a cube to a rectangular prism, and a cube to an asymmetric shape, shown in Figure 1. We use a 2-layer relaxed $E(3)$ NN with the network $l_{\text{max}} = 2$ and use relaxed weights up to $l_{\text{relaxed}} = 4$ with both even and odd parity in each layer ($\tilde{\theta} = 0_e \oplus 0_o \oplus 1_e \oplus 1_o \oplus 2_e \oplus 2_o \oplus 3_e \oplus 3_o \oplus 4_e \oplus 4_o$). We note that both the choice of the network l_{max} and l_{relaxed} is a hyperparameter. $l_{\text{max}} = 2$ is a standard choice for the network. We choose a higher l_{relaxed} to illustrate different learned symmetry breaking factors. To ensure that the learned symmetry breaking includes parity, both even and odd irreps should be included.

We analyze the learned relaxed weights using conventional symmetry analysis to confirm that the model learns the correct amount of symmetry breaking, following the same process as Smidt et al. (2021). First consider the case of transforming the cube to the rectangular prism. In 3D, the cube has symmetry group O_h , and the symmetry group of the rectangular prism is D_{4h} . Intuitively, for a cube, the x, y and z axes are symmetrically equivalent. However, in a rectangular prism, the x and y axes are symmetrically equivalent, and the z axis is unique. Thus, the relaxed weights should learn some scalar signal that demonstrates

¹When referring informally to the symmetry of a sample x we are referring to the stabilizer $\text{Stab}(x) = \{g \in G \mid g \cdot x = x\}$ or the set of symmetry operations that leave the shape fixed.

this relationship (i.e. $x^2 = y^2 \neq z^2$). We can calculate the learned scalar signals from the relaxed weights using Equation 8.

The learned relaxed weights for cube to rectangular prism are zero except for $\theta^{2,1}, \theta^{4,1}$, where we use the notation for irreps indexed by (l, p) . We can consider the scalar signal learned by $\theta^{2,1}$ using the analytic expression for the spherical harmonics given in the e3nn codebase. The specific non-zero relaxed weights correspond to $m = 0$ and $m = 2$, so we compute the scalar signal with spherical harmonics $Y_0^{2,1}, Y_2^{2,1}$, where the subscript denotes the m index. Computing the scalar signal $\theta_0^{2,1}Y_0^{2,1} + \theta_2^{2,1}Y_2^{2,1}$ yields a function of the form $ax^2 + ay^2 - 2az^2$ for each layer’s relaxed weights, demonstrating that the x and y axes are symmetrically equivalent but that the z axis is unique. In fact, the learned scalar signal corresponds exactly to a basis function for irrep E_g of O_h that is not present in D_{4h} (see Appendix A.1). The same computation holds for the learned $\theta^{4,1}$ relaxed weights. Thus, we find that either $\theta^{2,1}$ or $\theta^{4,1}$ breaks symmetry from the cube to the rectangular prism. Note that one may recover degenerate symmetry breaking factors as in this case, this degeneracy can be reduced by using a smaller l_{relaxed} or by adding a loss penalizing higher l weights (Smidt et al., 2021).

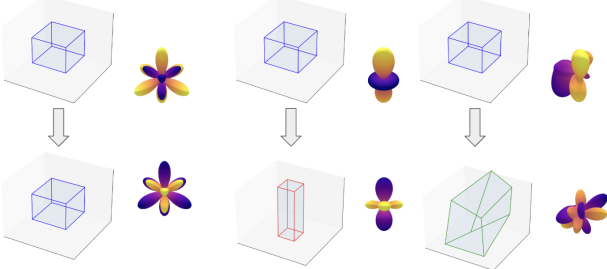


Figure 1. Visualization of tasks and corresponding spherical harmonic projections of the relaxed weights for the first (first row) and second (second row) layers. The spherical harmonic projections are plotted setting the scalar (0_e) term to zero for ease of viewing. A 2-layer relaxed $E(3)$ NN network is trained to 1) map a cube to a cube, 2) map a cube to a rectangular prism, and 3) map a cube to a less symmetric object.

In the case of mapping the cube to itself, we do not learn any relaxed weights for $l = 2$, thus preserving O_h symmetry. When transforming the cube to a random shape, all relaxed weights are non-zero, illustrating the lack of symmetry as seen in Figure 2. These experiments demonstrate the interpretability of the relaxed weights as spherical harmonic signals and that they illuminate the correct symmetry breaking factors.

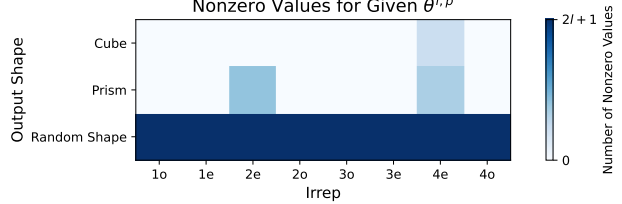


Figure 2. The number of nonzero values for each $\theta^{l,p}$ for the last layer in each network for the task of mapping the cube to a given output shape. Note that each irrep l has dimension $2l + 1$.

5.2. Charged Particle in an Electromagnetic Field

To illustrate a physical application of the relaxed $E(3)$ NN, we consider the trajectory of a charged particle in an electromagnetic field. The force on a charged particle in an electric field \vec{E} and a magnetic field \vec{B} is given by $\vec{F} = q(\vec{E} + \mathbf{v} \times \vec{B})$. \vec{E} is a vector (1_o) and \vec{B} is a pseudovector (1_e). Figure 3 presents an example of a positively charged particle trajectory with random initial position and velocity under an electric field in the \hat{x} direction and a magnetic field in the \hat{y} direction.

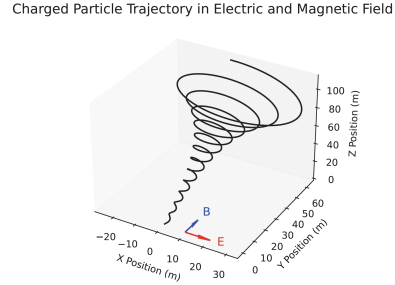


Figure 3. Sample trajectories of particles with random initial velocities and starting positions under an electric field in the \hat{x} direction and a magnetic field in the \hat{y} direction.

We thus consider if a relaxed $E(3)$ NN can discover the relationship between the electric and magnetic field—learning a 1_o vector with the correct magnitude and direction for \vec{E} and learning a 1_e pseudovector with the correct magnitude and direction for \vec{B} . For simplicity, we consider a single particle trajectory with $\vec{E} = [1, 0, 0]$ and $\vec{B} = [0, 1, 0]$ with a randomly initialized position and velocity. The network is adapted from a convolutional network for a graph with node/edge attributes (NetworkForAGraphWithAttributes included in e3nn).

We aim to predict the force on each particle given its velocity and thus include no coordinate information to the network. The input to the network is a single particle with a $1_o \oplus 0_e$ node attribute representing the particle velocity and the scalar charge. Note the even parity scalar charge is included

Model	Equiv	Relaxed
Training MSE	0.07	1e-6

Table 1. Training MSE for equivariant model and relaxed model when predicting electromagnetic forces for multiple timesteps in a trajectory. The relaxed model is able to overfit to the training set while the equivariant model remains in a non-symmetry breaking configuration.

to ensure the network can learn even irreps as well as odd. The desired output is the 1_o force acting on the particle at that timestep. We consider a 1-layer relaxed network with relaxed weights $0_e \oplus 0_o \oplus 1_o \oplus 1_e$. The network is then trained on multiple timesteps in the trajectory, predicting the force at each timestep.

We emphasize that through showing the model multiple timesteps with different velocity vectors, we break symmetry and allow the relaxed weights to learn the form of the electric and magnetic fields. An equivariant neural network with equivalent architecture without relaxed weights cannot accomplish this task, rather the loss remains “stuck” in a non-symmetry breaking configuration. The relaxed $E(3)$ NN learns the correct \vec{E} and \vec{B} fields, with error of approximately 0.001-0.01 in the y and z components after normalization as seen in Figure 4. This example illustrates the physical interpretability of the relaxed weights and their potential for application to more complicated physical examples.

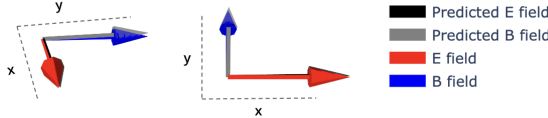


Figure 4. True and predicted fields for the relaxed network.

6. Discussion

We introduce a formulation for a relaxed $E(3)$ equivariant graph neural network and implement this in the e3nn framework. Using deformations of 3D shapes and analyzing the learned relaxed weights, we find that the relaxed weights learn the correct mathematical form of the symmetry breaking parameters. Given the physical example of a charged particle in an electromagnetic field, the relaxed $E(3)$ NN is able to learn the vector and pseudovector form of the electric and magnetic field. We aim to further characterize the mathematical properties of relaxed $E(3)$ NNs, apply them to more complicated examples in experimental physics and materials science, and study their optimization dynamics. For reproducibility, we include our code at <https://github.com/atomicarchitects/RelaxedE3NN>.

7. Acknowledgements

Elyssa Hofgard was supported by the U.S. Department of Energy, Office of Science, Office of Advanced Scientific Computing Research, Department of Energy Computational Science Graduate Fellowship under Award Number DE-SC0024386. Rui Wang and Tess Smidt were supported by DOE ICIDI grant DE-SC0022215. Robin Walters was supported by NSF 2134178. This research used resources of the National Energy Research Scientific Computing Center (NERSC) under Award Number ERCP0028753, a Department of Energy Office of Science User Facility.

This report was prepared as an account of work sponsored by an agency of the United States Government. Neither the United States Government nor any agency thereof, nor any of their employees, makes any warranty, express or implied, or assumes any legal liability or responsibility for the accuracy, completeness, or usefulness of any information, apparatus, product, or process disclosed, or represents that its use would not infringe privately owned rights. Reference herein to any specific commercial product, process, or service by trade name, trademark, manufacturer, or otherwise does not necessarily constitute or imply its endorsement, recommendation, or favoring by the United States Government or any agency thereof. The views and opinions of authors expressed herein do not necessarily state or reflect those of the United States Government or any agency thereof.

References

Character of a Representation, pp. 29–55. Springer Berlin Heidelberg, Berlin, Heidelberg, 2008. doi: 10.1007/978-3-540-32899-5_3. URL https://doi.org/10.1007/978-3-540-32899-5_3.

Batzner, S., Musaelian, A., Sun, L., Geiger, M., Mailoa, J. P., Kornbluth, M., Molinari, N., Smidt, T. E., and Kozinsky, B. E(3)-equivariant graph neural networks for data-efficient and accurate interatomic potentials. *Nat. Commun.*, 13(1):2453, May 2022.

Cohen, T. S. and Welling, M. Steerable CNNs. *arXiv preprint arXiv:1612.08498*, 2016.

Fang, S., Geiger, M., Checkelsky, J. G., and Smidt, T. Phonon predictions with E(3)-equivariant graph neural networks. *arXiv preprint: arXiv:2403.11347*, 2024. URL <https://arxiv.org/abs/2403.11347v1>.

Frey, N. C., Soklaski, R., Axelrod, S., Samsi, S., Gómez-Bombarelli, R., Coley, C. W., and Gadepally, V. Neural scaling of deep chemical models. *Nature Machine Intelligence*, 5(11):1297–1305, October 2023.

Geiger, M. and Smidt, T. e3nn: Euclidean neural networks. *arXiv preprint arXiv:2207.09453*, 2022.

Geiger, M., Smidt, T., M., A., Miller, B. K., Boomsma, W., Dice, B., Lapchevskyi, K., Weiler, M., Tyszkiewicz, M., Batzner, S., Madisetti, D., Uhrin, M., Frellsen, J., Jung, N., Sanborn, S., Wen, M., Rackers, J., Rød, M., and Bailey, M. Euclidean neural networks: e3nn, April 2022. URL <https://doi.org/10.5281/zenodo.6459381>.

Gelessus, A. Character table for point group d4h, 2023a. URL <http://symmetry.jacobs-university.de/cgi-bin/group.cgi?group=604&option=4>.

Gelessus, A. Character table for point group oh, 2023b. URL <http://symmetry.jacobs-university.de/cgi-bin/group.cgi?group=904&option=4>.

Kondor, R. N-body networks: a covariant hierarchical neural network architecture for learning atomic potentials. March 2018.

Landau, L. The theory of phase transitions. *Nature*, 138 (3498):840–841, 1936.

Liao, Y.-L., Wood, B., Das, A., and Smidt, T. Equiformer2: Improved equivariant transformer for scaling to higher-degree representations. *arXiv preprint arXiv:2306.12059*, 2023.

McNeela, D. Almost equivariance via lie algebra convolutions. *arXiv preprint arXiv:2310.13164*, 2023.

Owen, C. J., Torrisi, S. B., Xie, Y., Batzner, S., Coulter, J., Musaelian, A., Sun, L., and Kozinsky, B. Complexity of Many-Body interactions in transition metals via Machine-Learned force fields from the TM23 data set. February 2023.

Rackers, J. A., Tecot, L., Geiger, M., and Smidt, T. E. A recipe for cracking the quantum scaling limit with machine learned electron densities. *Mach. Learn.: Sci. Technol.*, 4(1):015027, February 2023.

Smidt, T. E., Geiger, M., and Miller, B. K. Finding symmetry breaking order parameters with euclidean neural networks. *Physical Review Research*, 3(1):L012002, 2021.

Tagawa, T. Symmetry in fluid flow, 2023.

Thomas, N., Smidt, T., Kearnes, S., Yang, L., Li, L., Kohlhoff, K., and Riley, P. Tensor field networks: Rotation-and translation-equivariant neural networks for 3d point clouds. *arXiv preprint arXiv:1802.08219*, 2018.

Wang, R., Walters, R., and Yu, R. Approximately equivariant networks for imperfectly symmetric dynamics. In *International Conference on Machine Learning*, pp. 23078–23091. PMLR, 2022.

Wang, R., Hofgard, E., Walters, R., and Smidt, T. Discovering symmetry breaking in physical systems with relaxed group convolution. *arXiv preprint arXiv:2310.02299*, 2024.

Weiler, M., Geiger, M., Welling, M., Boomsma, W., and Cohen, T. 3d steerable cnns: Learning rotationally equivariant features in volumetric data. In *NeurIPS*, 2018.

Zee, A. *Group theory in a nutshell for physicists*. In a nutshell. Princeton University Press, 2016. ISBN 978-0-691-16269-0. URL <https://books.google.com/books?id=FWkujgEACAAJ>. tex.lccn: 2015037408.

O_h	E	$8C_3$	$6C_2$	$6C_4$	$3C_2 = (C_4)^2$	i	$6S_4$	$8S_6$	$3\sigma_h$	$6\sigma_d$	linear functions, rotations	quadratic functions	cubic functions
A_{1g}	+1	+1	+1	+1	+1	+1	+1	+1	+1	+1	-	$x^2 + y^2 + z^2$	-
A_{2g}	+1	+1	-1	-1	+1	+1	-1	+1	+1	-1	-	-	-
E_g	+2	-1	0	0	+2	+2	0	-1	+2	0	-	$(2z^2 - x^2 - y^2, x^2 - y^2)$	-
T_{1g}	+3	0	-1	+1	-1	+3	+1	0	-1	-1	(R_x, R_y, R_z)	-	-
T_{2g}	+3	0	+1	-1	-1	+3	-1	0	-1	+1	-	(xz, yz, xy)	-
A_{1u}	+1	+1	+1	+1	+1	-1	-1	-1	-1	-1	-	-	-
A_{2u}	+1	+1	-1	-1	+1	-1	+1	-1	-1	+1	-	xyz	-
E_u	+2	-1	0	0	+2	-2	0	+1	-2	0	-	-	-
T_{1u}	+3	0	-1	+1	-1	-3	-1	0	+1	+1	(x, y, z)	-	$(x^3, y^3, z^3) x(z^2 + y^2), y(z^2 + x^2), z(x^2 + y^2)$
T_{2u}	+3	0	+1	-1	-1	-3	+1	0	+1	-1	-	-	$[x(z^2 - y^2), y(z^2 - x^2), z(x^2 - y^2)]$

 Table 2. Character table for point group O_h (Gelessus, 2023b).

D_{4h}	E	$2C_4(z)$	C_2	$2C'_2$	$2C_2$	i	$2S_4$	σ_h	$2\sigma_v$	$2\sigma_d$	linear functions, rotations	quadratic functions	cubic functions
A_{1g}	+1	+1	+1	+1	+1	+1	+1	+1	+1	+1	-	$x^2 + y^2, z^2$	-
A_{2g}	+1	+1	+1	-1	-1	+1	+1	+1	-1	-1	R_z	-	-
B_{1g}	+1	-1	+1	+1	-1	+1	-1	+1	+1	-1	-	$x^2 - y^2$	-
B_{2g}	+1	-1	+1	-1	+1	+1	-1	+1	-1	+1	-	xy	-
E_g	+2	0	-2	0	0	+2	0	-2	0	0	(R_x, R_y)	(xz, yz)	-
A_{1u}	+1	+1	+1	+1	+1	-1	-1	-1	-1	-1	-	-	-
A_{2u}	+1	+1	+1	-1	-1	-1	-1	-1	+1	+1	z	-	$z^3, z(x^2 + y^2)$
B_{1u}	+1	-1	+1	+1	-1	-1	+1	-1	-1	+1	-	-	xyz
B_{2u}	+1	-1	+1	-1	+1	-1	+1	-1	+1	-1	-	-	$z(x^2 - y^2)$
E_u	+2	0	-2	0	0	-2	0	+2	0	0	(x, y)	-	$(xz^2, yz^2) (xy^2, x^2y), (x^3, y^3)$

 Table 3. Character table for point group D_{4h} (Gelessus, 2023a).

A. Symmetry Analysis for Experiment 5.1

A.1. Character Tables

We present an overview of character tables used for the symmetry analysis in Section 5.1. Character tables are used for finite groups (subgroups of $E(3)$) and are used extensively in solid state physics, crystallography, and chemistry. See Dre (2008); Zee (2016) for more information on group and representation theory in physics and materials.

Classes and character. Given a group G , two elements g and g' are conjugate if there exists another element $x \in G$ such that $g' = x^{-1}gx$. A class is the set of group elements that can be obtained from a given element $g \in G$ by conjugation. The elements of a given group can thus be divided into classes. Classes correspond to physically distinct kinds of symmetry (Dre, 2008) and are thus useful for categorizing different symmetries of a material rather than enumerating all individual group elements. Examples of classes are the twofold axes of rotation of an equilateral triangle or the threefold rotations. These classes can be related to the character of a given representation. Let V be a finite-dimensional vector space and consider $D : G \rightarrow \text{GL}(V)$, a representation of G on V . The character of $D(g)$ is the trace of the matrix of the representation, $\text{Tr}(D(g))$. One can show that the character for each element in a class is the same (Dre, 2008). As the character for each element in a class is the same, this provides a useful way to connect group representations to sets of physically distinct symmetries.

The relationship between characters of representations and classes for a given group can be summarized in a character table. The left hand column labels the irreps and the top row labels the class. Notation used in character tables can vary, with Schoenflies symmetry notation commonly used to describe molecular symmetries and Hermann-Mauguin notation commonly used in crystallography. For the purposes of this analysis, it is not necessary to be familiar with this notation, but the interested reader may consult Chapter 3 in Dre (2008). The entries correspond to the characters of different irreps. On the right-hand side, the columns list basis functions corresponding to irreps —functions that can be used to generate matrices of given irreps and transform the same way as that irrep.

Character tables for different groups can then be compared to find which irreps break symmetries between groups. For example, in Section 5.1, we consider deforming a cube with symmetry group O_h to a rectangular prism with symmetry group D_{4h} . For O_h , the character table in Table 2 shows that irrep E_g has basis functions of $2z^2 - x^2 - y^2$ (highlighted in blue) and $x^2 - y^2$. For D_{4h} , the basis function of $2z^2 - x^2 - y^2$ is not present for any of the irreps. However, irrep B_{1g} has a basis function of $x^2 - y^2$. This implies that the basis function $2z^2 - x^2 - y^2$ for irrep E_g can be used to break symmetry

	$\theta_0^{2,1}$	$\theta_2^{2,1}$	x^2	y^2	z^2
Layer 0	0.0031	-0.0054	0.007	0.007	-0.014
Layer 1	0.33	-0.57	0.73	0.73	-1.45

Table 4. Relaxed weights and calculated coefficients from the scalar signal for x^2 , y^2 , and z^2 .

between O_h and D_{4h} , but that the model should preserve $x^2 = y^2$.

A.2. Converting Relaxed Weights to Spherical Signal

For the shape deformation experiments in Section 5.1, we give the analytic forms of the spherical harmonics in e3nn. For the cube to rectangular prism, the learned relaxed weights for $\theta^{2,1}$ and $\theta^{4,1}$. For $\theta^{2,1}$, the non-zero relaxed weights are $\theta_0^{2,1}$ and $\theta_2^{2,1}$, corresponding to spherical harmonics

$$Y_0^{2,1} = \sqrt{5} \left(y^2 - \frac{1}{2} (x^2 + z^2) \right), Y_2^{2,1} = \frac{1}{2} \sqrt{15} (z^2 - x^2)$$

For a given model, we can then compute the scalar signal $f_0^2 = \theta_0^{2,1} Y_0^{2,1} + \theta_2^{2,1} Y_2^{2,1}$ for each layer, as seen in Table 4. Note that the specific numerical values may change across layers/model initializations, yet they yield a scalar function of the form $ax^2 + ay^2 - 2az^2$, demonstrating that the basis function for irrep E_g is used to break symmetry while retaining $x^2 = y^2$ (note multiplying the basis function by -1 does not change the symmetry properties). A similar (but more involved) analysis can be done for relaxed weights $\theta^{4,1}$ to show that they also preserve D_{4h} symmetry and transform as the irrep E_g .

B. Experimental Details

We provide additional details for each experiment.

B.1. Shape Deformations

The objective is the MSE loss between the predicted spherical harmonic projections and the spherical harmonic projections of the vertices of the output shape. We use the SGD optimizer with a learning rate of 5e-3. The relaxed weights are also regularized throughout training by the L_2 norm with

$$\lambda \sum_{\substack{0 \leq l \leq l_{\max} \\ p \in \{1, -1\}}} \|\theta^{l,p}\|_2 \quad (9)$$

where we set $\lambda = 1e - 6$ in order to provide a slight bias towards equivariance. Each model is trained for 2,500 epochs.

B.2. Particle in Electromagnetic Field

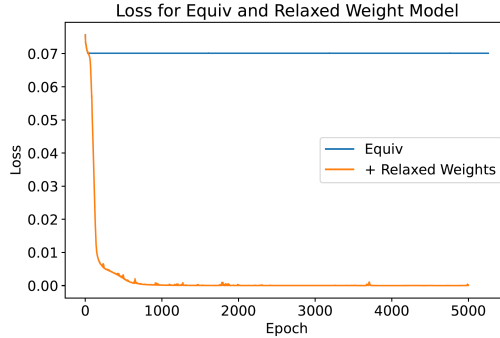


Figure 5. Loss for fully equivariant model and model with relaxed weights trained on the same task.

We include no positional information to the network, so there are no edge attributes. The convolution over a single particle is still well-defined assuming a self-interaction edge is included in the network (reducing to an equivariant MLP where the

irreps interact through the nonlinearities). The node inputs for each timestep are irreps $0_e \oplus 0_o \oplus 1_e \oplus 1_o \oplus 2_e \oplus 2_o$ with only the scalar term non-zero. Including higher order irreps allows for more paths in the tensor product and more model expressivity.

We consider 500 timesteps from a single trajectory and train with a batch size of 50. We use the Adam optimizer with a learning rate of 1e-3. The model is trained for 5,000 epochs with the MSE loss between the predicted and true forces. The relaxed weights are also regularized by Equation 9 where we set $\lambda = 1e - 4$. We show that an equivariant model cannot accomplish this task as it requires symmetry breaking. We plan to make our code publically available with further experiments.